Viscoelasticity of Solutions of Motile Polymers

T. B. Liverpool,[1,2] A. C. Maggs,[1] and A. Ajdari[1]

[1]*Physico-Chimie Theorique, ESA CNRS 7083, E.S.P.C.I., 75231 Paris Cedex 05, France*

[2]*Condensed Matter Theory Group, Blackett Laboratory, Imperial College, London SW7 2BZ, United Kingdom*

(Received 24 November 2000)

We explore the linear viscoelastic response of an entangled, isotropic solution of polar semiflexible polymers with *active, motile* centers which generate longitudinal motion. Because of the activity of these centers, the short-time modulus displays two novel power-law regimes: Initially $G(t) \propto t^{-1/8}$, then the response is "Rouse-like" with $G(t) \propto t^{-1/2}$. At longer times we find accelerated relaxation due to directed reptation, resulting in a reduced low frequency viscosity.

DOI: 10.1103/PhysRevLett.86.4171 PACS numbers: 87.16.Ka, 61.25.Hq, 83.60.Bc, 87.15.La

The proteins myosin and actin are major components of the cell cytoskeleton. Myosin, a molecular motor, hydrolyzes adenosine triphosphate (ATP) to generate directional forces and motion along polar actin filaments (F-actin) [1]. In vitro experiments have shown that the addition of ATP to a solution of actin filaments and myosin can lead to abrupt changes (e.g., liquefaction) in its behavior [2]. Out of equilibrium chemical activity in motor-filament solutions is known to lead to complex cooperative behavior [3–5] including pattern formation and creation of dissipative structures. However, even in the *absence* of macroscopic patterning the mechanical response functions of such a mixture should be strongly modified by the novel microscopic dynamics occurring in motor/filament solutions.

Myosin spontaneously aggregates in vitro to form clusters. In an ATP rich system these myosin clusters can then bind to pairs of filaments and actively move the filaments with respect to each other. In a sheared sample this results in rapid release of elastic strains, for the directed motion of the polymers leads to a reduction of the reptation time from $t_{\text{rept}} \sim L^3$ (characteristic of diffusion) to $t_{\text{rept}} \sim L$ for filaments of length L sliding at constant speed [2,6]. Motivated by experimental observations and this simple argument, one is led to ask a number of further *quantitative* questions. What is the elastic stress supported by such a system? What are the relevant relaxation mechanisms and time scales? As a step in this direction, we focus here on a simple model for the viscoelasticity of an "active" solution of motile semiflexible filaments, within the "tube" picture of polymer dynamics. This is clearly an oversimplification of the in vitro system described above; nevertheless, the physics of the problem, even with this approximation, is interesting and nontrivial.

We consider a monodisperse solution of semiflexible and polar polymers of persistence length L_p, length L, and diameter a, with $L_p \gg a$, at a monomer concentration ρ_a such that the mesh size of the solution is $\xi \simeq (\rho_a a)^{-1/2} \ll L_p, L$ [7]. We model the ATP induced activity of actin clusters by stochastic forces on the polymers, *parallel to the filament contour* (transverse motion is constrained by entanglements), which always act in the same direction with respect to the polarity of the filaments. The effect of the motor activity is (1) to increase the amplitude of the *longitudinal* fluctuations along the contour of the filaments giving rise to a higher *effective* temperature $T \to T + T_{\text{act}}$ for the tangential motion and (2) to give the filaments a nonzero curvilinear drift velocity in their tubes, v_m. Increasing/decreasing activity leads to an increase/decrease in T_{act} and v_m. A cartoon of the system is shown in Fig. 1. We note that similar descriptions in terms of an effective temperature for a nonequilibrium system have been used to model noise in foams [8] as well as other driven, glassy systems.

We derive the linear viscoelastic response of such an *active* polymer solution, assuming that its structure is not perturbed by the activity of the motor clusters. Despite this crude assumption we uncover rich physical behavior, as the "activity" modifies the already subtle dynamics of *passive* semiflexible polymer solutions [9–13]. We first summarize our main results. We then describe our model, our calculation strategy, and the various scaling regimes obtained. Finally we return to the actin-myosin system, discuss the magnitude of the effects, and emphasize elements neglected in the present model.

Main results.—The linear response of this polymer solution to a weak time dependent shear strain, $\gamma_{ij}(t)$, is characterized by the shear modulus $G(t)$, such that the shear

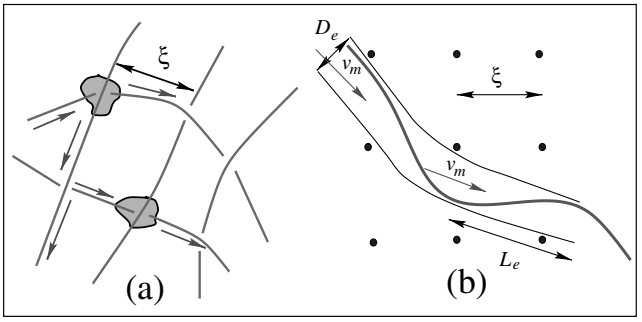

FIG. 1. (a) The active solution with motor centers and entanglement points. (b) The "tube" encircling the polymer and the directed motion v_m. We show the lengths ξ, L_e, D_e.

stress is $\boldsymbol{\sigma}_{ij}(t) = \int_{-\infty}^{t} dt'\, G(t - t')\dot{\boldsymbol{\gamma}}_{ij}(t')$ [7]. We find short-time (high frequency) moduli as well as terminal relaxation times that differ from those of passive polymer solutions. The *active* solution is harder at high frequencies due to the increased fluctuations of the longitudinal modes. These *also* change the relative magnitude of the longitudinal and transverse fluctuations, leading to two new relaxation regimes. At very low frequencies, the directed motion of the filaments leads to a softening or "fluidification" as suggested in the introduction. Our results are schematized in Fig. 2 and summarized as follows. Upon submitting the system to a step shear, the shear modulus $G(t)$ decays for very short times as $t^{-3/4}$, as for passive polymer solutions [12,13]. This holds up to a time $t_0 \sim (1 + T_{\rm act}/T)^{-8/5} L_p^3 \eta/k_B T$ where we find a regime with two new power-law decays: $G(t) \sim t^{-1/8}$ up to a time $t_1 \sim \eta L_p^{-1/5} \xi^{16/5}/k_B T$ and a modulus $G_2 \sim k_B(T + T_{\rm act}) \xi^{-12/5} L_p^{-3/5}$, after which there is a faster decay $G(t) \sim t^{-1/2}$ (η is the solvent viscosity). In the long-time regime, the relaxation modulus develops a plateau, as *trapped* stress cannot relax due to entanglements before the filaments escape from their initial tubes [7]. While the magnitude of the plateaux are the same as for passive polymer solutions, the tube renewal time has a different dependence on chain length L and persistence length L_p. When $L/L_p \gg 1$, the dominant stress is due to constrained transverse fluctuations of the filament [9,10,12] leading to a plateau of magnitude $G_3 \sim \xi^{-14/5} k_B T/L_p^{1/5}$ which begins at a time $t_2^{\rm coil} \sim L_p^3 (\xi/L_p)^4 (1 + T_{\rm act}/T)^2 \eta/k_B T$, and decays after a time $t_3 \simeq L/v_m$. For filaments with $L/L_p \ll 1$, the stress is due to constrained orientational dynamics [12,14–16] and from $t_2^{\rm rod} \sim L^2 L_p (\xi/L_p)^{12/5} (1 + T_{\rm act}/T)^2 \eta/k_B T$ we find a plateau of magnitude $G_4 \sim k_B T \xi^{-2} L^{-1}$ which decays after a time $t_4 \simeq \sqrt{L L_p}/v_m$.

Explicit analysis.—The stress is calculated from the fluctuating dynamics of Kratky-Porod worm-like chains. A *typical* filament conformation is parametrized by $\mathbf{R}(s)$. The Hamiltonian of a worm-like chain is given by $\mathcal{H}_{wlc}[\mathbf{R}(s), \tau(s)] = \kappa/2 \int_0^L ds\, |\partial_s^2 \mathbf{R}|^2 + \int_0^L ds\, \tau(s) \times (|\partial_s \mathbf{R}|^2 - 1)$ where $\partial_x A \equiv \partial A/\partial x$ and an instantaneous local tension, $\tau(s)$, is induced by the incompressibility of the chain. The persistence length $L_p = \kappa/k_B T$ is the length scale over which the chain loses memory of its orientation. The filaments are confined to a tube [7] of diameter $D_e \sim L_p (\xi/L_p)^{6/5}$. We define an entanglement (deflection) length [14–16] $L_e \sim L_p (\xi/L_p)^{4/5}$, the distance between successive collisions of the filament with its tube [see Fig. 1(b)]. The hierarchy of length scales is $L, L_p \gg L_e \gg a$. On length scales ℓ less than L_e, the relaxation is due to the dynamics of "free" chains [7], while for $\ell > L_e$ it is due to diffusive directed motion of the polar filaments in their tubes. For $\ell < L_e$ (and consequently $\ell < L_p$), the chain conformation is anisotropic and can be described by an expansion about a rod with orientation $\hat{\mathbf{u}}$ (a unit vector, $|\hat{\mathbf{u}}|^2 = 1$), $\mathbf{R}(s,t) = [s - r_\parallel(s,t)]\hat{\mathbf{u}} + \mathbf{r}_\perp(s,t)$; $\hat{\mathbf{u}} \cdot \mathbf{r}_\perp(s,t) \equiv 0$ with parallel (longitudinal) and perpendicular (transverse) components of motion, $r_\parallel$, $|\mathbf{r}_\perp| \ll s$. The filament dynamics in a shear flow are described by the equations [17]

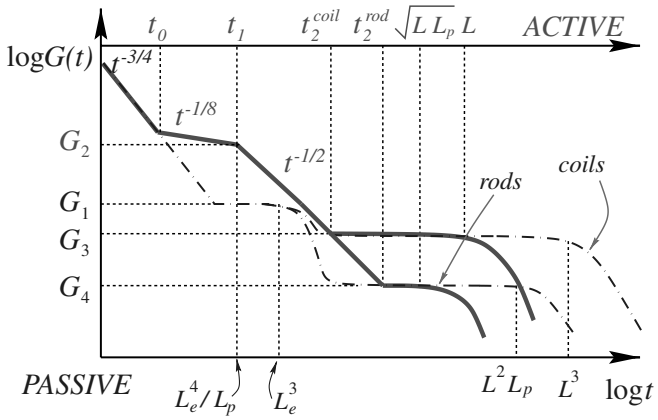

FIG. 2. Shear modulus as a function of time t: comparison of active (thick-solid lines) and passive (thin-dashed lines) solutions. The different regimes separated by t_0, t_1, $t_2^{\rm coil}$, $t_2^{\rm rod}$, t_3, and t_4, respectively. Top: Time scale for active solutions. Bottom: Time scale for passive solutions.

$$\partial_t \mathbf{r}_\perp(s,t) = \zeta_\perp^{-1}[-\kappa \partial_s^4 \mathbf{r}_\perp + \tau(s,t)\partial_s^2 \mathbf{r}_\perp + \partial_s \tau \partial_s \mathbf{r}_\perp + \mathbf{f}_\perp(s,t)] + (\mathbf{I} - \hat{\mathbf{u}}\hat{\mathbf{u}}) \cdot \dot{\boldsymbol{\gamma}}(t) \cdot \mathbf{r}_\perp + O(|\partial_s \mathbf{r}_\perp|^3), \quad (1)$$

$$\partial_t r_\parallel(s,t) = \zeta_\parallel^{-1}[-\kappa \partial_s^4 r_\parallel - \partial_s \tau + f_m(s,t) + f_\parallel(s,t)] + \dot{\boldsymbol{\gamma}}_{ij}(t)\hat{u}_i \hat{u}_j (r_\parallel - s) + O(|\partial_s \mathbf{r}_\perp|^3). \quad (2)$$

Note the anisotropic nature of the coupling to the shear flow due to the rodlike nature of the polymer. Because of constraint of constant length, $\partial_s r_\parallel = \frac{1}{2}|\partial_s \mathbf{r}_\perp|^2 + O(|\partial_s \mathbf{r}_\perp|^4)$ which determines τ, these equations are coupled. The friction coefficients are $\zeta_\parallel = 2\pi\eta \log|\xi/a| = \frac{1}{2}\zeta_\perp$. For short filaments $L < L_p$, the rotational diffusion of a rod of length L determines the dynamics of $\hat{\mathbf{u}}(t)$ which is much slower than that of $r_\parallel, \mathbf{r}_\perp$ with friction coefficient $\zeta_{\mathbf{u}} \simeq \pi\eta L^3$. We have in addition to the thermal fluctuating force $(f_\parallel(s,t), \mathbf{f}_\perp(s,t))$ a *nonequilibrium* or *active* force, $f_m(s,t)$, in the *longitudinal* direction due to the activity of the motors. The thermal force has zero mean, $\langle \mathbf{f}(s,t) \rangle = 0$, and mean square fluctuations $\langle f_i(s,t) f_j(s',t') \rangle = 2k_B T \delta_{ij} \zeta_i \delta(s - s') \delta(t - t')$ where the subscripts $\{i\}$ refer to $\parallel, \perp$. We choose to model the active force by a nonzero mean $\langle f_m(s,t) \rangle = \zeta_\parallel v_m$ and mean square fluctuations of the form, $\delta f_m(s,t) = f_m(s,t) - \langle f_m(s,t) \rangle$, $\langle \delta f_m(s,t) \delta f_m(s',t') \rangle = 2k_B T_{\rm act} \zeta_\parallel \delta(s - s') \times \delta(t - t')$, giving an active contribution, $T_{\rm act}$, to the "temperature" of the longitudinal motion. A self-consistent description [17] of the dynamics can be obtained from the

solution of Eqs. (1) and (2) and inextensibility. Because the transverse dynamics is cut off at L_e, there is different behavior at high and low frequencies with a crossover frequency, $\omega_e = 2\alpha\pi/L_e^4$ ($\alpha = \kappa/\zeta_\perp$). The dynamic fluctuations of semiflexible filaments are anisotropic [17,18]. After time t, longitudinal fluctuations are relaxed over a length $\ell_\parallel(t) = [tk_BT(2L_p)^5/2\pi\eta]^{1/8}$ for $t < 1/\omega_e$ and $\ell_\parallel(t) = (tk_BTL_p^2L_e^{-3}/2\pi\eta)^{1/2}$ for $t > 1/\omega_e$. In comparison, transverse fluctuations are relaxed over a length $\ell_\perp(t) = (tk_BTL_p/4\pi\eta)^{1/4}$ for $t < 1/\omega_e$ [17] and can relax only by reptation for $t > 1/\omega_e$.

We calculate the Kramers-Kirkwood stress tensor [7], $\boldsymbol{\sigma}_{ij}(t) = -\rho_a/L \int_0^L ds\,\langle F_i(s,t)R_j(s,t)\rangle$ where $\mathbf{F}(s,t)$ is the *total* force on the filament at arc length s at time t, and $\mathbf{R}(s,t) = (s - r_\parallel)\hat{\mathbf{u}} + \mathbf{r}_\perp$ is the position of the filament. The force balance equations (1) and (2) and the rotational dynamics give $\mathbf{F}(s,t)$. After subtracting the minor contributions and the isotropic part of the stress, we obtain

$$\boldsymbol{\sigma}_{ij}(t) \simeq \left\langle \frac{\rho_a}{\ell}\int_0^{\ell\sim L_p} ds\left\{\hat{u}_i\hat{u}_j\Big(\underbrace{s\partial_s\tau}_{\sigma^{(1)}} - \underbrace{r_\parallel\partial_s\tau}_{\sigma^{(2)}}\Big) - \underbrace{\kappa\partial_s^4 r_{\perp i}r_{\perp j} + \partial_s(\tau\partial_s r_{\perp i})r_{\perp j}}_{\sigma^{(3)}}\right\} + \underbrace{3\frac{\rho_a a}{L}k_BT\Big(\hat{u}_i\hat{u}_j - \frac{1}{3}\delta_{ij}\Big)}_{\sigma^{(4)}}\right\rangle, \tag{3}$$

where the average is over thermal and active fluctuations and orientation. Three of the four contributions to the shear stress, $\sigma_{ij}^{(1,3,4)}$, arise from the coupling of the strain to $r_\parallel$, $\mathbf{r}_\perp$, and $\hat{\mathbf{u}}$, respectively. They have been analyzed recently for *passive* solutions [9–13], and named tension, curvature, and orientational stress, respectively. The term $\sigma_{ij}^{(2)} = -\langle\frac{\rho_a}{\ell}\int_0^{\ell\sim L_p} ds\, r_\parallel\partial_s\tau\rangle$, which we call the *longitudinal* stress is new. It has been ignored in passive polymer solutions, $T_{\rm act} = 0$, for it is then much smaller than the other three. In active polymer solutions, however, for large enough motor activity, i.e., $T_{\rm act}/T > (L_p/L_e)^{5/2} - 1$, it dominates the high frequency response.

High frequency behavior.—For short times, the filaments do not feel the confining interactions of entanglements. As activity does not couple to transverse modes, the tension modulus is the same as for passive polymer solutions, $G^{(1)}(t) \simeq \frac{\xi^{-2}k_BTL_p^2}{(tL_pk_BT/\zeta_\perp)^{3/4}} \simeq k_BT\xi^{-2}L_p^2/\ell_\perp^3(t)$. So are the curvature and orientation stresses, $G^{(3)}(t) \simeq \frac{\xi^{-2}k_BT}{(tL_pk_BT/\zeta_\perp)^{1/4}} \simeq \xi^{-2}k_BT/\ell_\perp(t)$ and $G^{(4)}(t) = \frac{3k_BT}{5L}\times\xi^{-2}e^{-6tk_BT/\zeta_u}$. The longitudinal modulus is given by $G^{(2)}(t) \simeq \frac{\xi^{-2}k_B(T+T_{\rm act})}{[t(2L_p)^5k_BT/\zeta_\parallel]^{1/8}} \simeq k_B(T + T_{\rm act})\xi^{-2}/\ell_\parallel(t)$. A simple explanation for this expression is as follows: after time t, divide the filaments into lengths (blobs) $\ell_\parallel(t)$ [compared to $\ell_\perp(t)$ for the curvature stress] with relaxed longitudinal fluctuations. Then, assuming affine deformation, the longitudinal stress is due to $k_B(T + T_{\rm act})$ (compared to k_BT for transverse) of stored energy per length $\ell_\parallel(t)$. At extremely short times the tension modulus $G^{(1)}(t) \sim t^{-3/4}$ is very high and dominates, but it relaxes much faster than the longitudinal modulus $G^{(2)}(t)$, which, for large $T_{\rm act}$, becomes the dominant component after t_0 defined by $G^{(2)}(t_0) = G^{(1)}(t_0)$. If the solution *activity* goes down, i.e., $T_{\rm act} \to 0$, $G^{(2)} \ll G^{(1)}$ [12,13] and this regime vanishes. As discussed in the following, $G^{(3,4)}$ become relevant only at longer times [9,12,14–16].

Intermediate frequency behavior.—At longer time scales ($t > t_1 \sim 1/\omega_e \sim \zeta_\perp L_e^4/k_BTL_p$), the filament dynamics starts to be affected by the confining effects of neighboring chains. Since the dominant component of the modulus $G^{(2)}$ is due to $r_\parallel$, it is there that we first see this effect. Solving Eq. (2) for $t > t_1$, we obtain a new power-law decay $G^{(2)}(t) \simeq \frac{\xi^{-2}k_B(T+T_{\rm act})}{(t\pi^3L_p^2k_BT/L_e^3\zeta_\parallel)^{1/2}} \simeq \xi^{-2}k_B(T + T_{\rm act})/\ell_\parallel(t)$, again due to nonrelaxed stress above the scale $\ell_\parallel(t)$. The modulus $G(t) \simeq G^{(2)}(t)$, until it becomes comparable to the plateaux of $G^{(3,4)}(t)$ at times $t_2^{\rm coil}$ and $t_2^{\rm rod}$, respectively.

Low frequency behavior.—For time scales larger than $t_\perp \simeq t_1$ [where $\langle\mathbf{r}_\perp(t_\perp)^2\rangle \simeq D_e^2$] and $t_u \sim \zeta_uD_e^2/k_BTL^2$, respectively, the transverse and orientational modes of the polymers feel the tube. Then the stress components $\boldsymbol{\sigma}^{(3,4)}(t)$ can relax only when the filament has moved out of its deformed original tube. The magnitude of the corresponding plateaux is the amount of nonrelaxed stress at the times $t_\perp$ (t_u) after a small step strain. As the motors give a mean velocity v_m to the filaments in their tubes, the filament dynamics obeys a diffusion equation with drift. We now discuss separately coil-like (a) and rod-like (b) filaments [12].

(a) Coils ($L \gg L_p$): For this system, stress is dominated at long times by the constraints on the transverse motion of the filament in its tube, i.e., $\sigma^{(3)}(t)$, which is proportional to the remaining amount of the original tube. This gives the relaxation modulus (valid until $t \sim L/v_m$), $G^{(3)}(t) = G_3\sum_{p,\rm odd}\frac{8}{p^2\pi^2}\cos(\frac{p\pi v_mt}{L})e^{-tp^2\pi^2D_c/L^2}$, where $G_3 = 2^{3/4}\Gamma(5/4)a\rho_ak_BT/3\pi L_e$ is the amount of curvature stress relaxed at $t_\perp$ and $D_c = k_B(T + T_{\rm act})/\zeta_\parallel L$ is the curvilinear diffusion constant along the tube axis. This is similar to the Doi-Edwards relaxation spectrum [7] but modulated by a cosine. For active polymer solutions $v_m/L \gg D_c/L^2$, and the relaxation time is $t_3 \sim L/v_m$. Making the solution less active, $v_m, T_{\rm act} \to 0$, we obtain the reptation result $t_3 \sim \zeta_\perp L^3/k_BT$ [7,9,12].

(b) Rods ($L \ll L_p$): For rod-like filaments, the dominant component of stress at long times is due to constrained orientational dynamics, i.e., $\sigma^{(4)}(t)$. For initially randomly oriented filaments, we obtain a relaxation modulus (valid until $t \sim L/v_m$) $G^{(4)}(t) \simeq G_4\cos(q_1v_mt)e^{-tq_1^2D_c}$,

where $G_4 = 3a\rho_a/5L \exp(-t_u 6k_B T\zeta_u) \sim 3a\rho_a/5L$ is the amount of stress relaxed at t_u and $q_1 = \sqrt{6/LL_p}$. For active solutions $v_m/L \gg D_c/LL_p$ and the relaxation time is $t_4 \sim \sqrt{LL_p}/v_m$. Decreasing the activity of the system, $v_m, T_{\text{act}} \to 0$, we recover the reptation result $t_4 \sim \zeta_\perp L^2 L_p/k_B T$ [12,14–16].

Discussion.—Let us return now to the actin-myosin-ATP system that stimulated our theoretical study: We estimate typical time scales and moduli from a direct mapping of our calculation onto this system. We have modeled the noise as a Gaussian white noise of nonzero mean. In a slightly more realistic picture, a motor center has periods of activity of duration t_s (the power stroke) during which a constant force f_0 is applied, separated by passive periods which are Poisson distributed with a mean duration αt_s; $\alpha \gg 1$. The motor clusters are also assumed randomly distributed along the filaments at a mean distance ℓ_m. Assuming that clusters act independently, we estimate from the mean force $v_m \simeq (1 + \alpha)^{-1} f_0/\zeta_\parallel \ell_m$, and from the local fluctuations of the force about its mean $k_B T_{\text{act}} \simeq f_0^2 t_s \alpha/(1 + \alpha)\zeta_\parallel \ell_m$. If myosin is at a concentration ρ_m and the mean number of myosin per cluster is N, then $\ell_m \sim N(\rho_m \xi^2)^{-1}$. Let us turn to numbers: a bound myosin has a power stroke of duration $t_s \simeq 5$ ms, a step size of $d_s \simeq 10$ nm, and a stall force of $f_{\max} \simeq 4$ pN [1]. By considering viscous drag, we estimate $f_0 \simeq 0.1$ pN $\ll f_{\max}$. Actin has persistence length $L_p \simeq 17$ μm and diameter $a \simeq 7$ nm. A solution of F-actin at a typical concentration 100 μg/ml has a mesh size $\xi \sim 0.5$ μm. For $\rho_m = 0.1$ μM (micromolar) and $N \simeq 10$ we estimate $\ell_m \sim 5$ μm. This gives $T_{\text{act}}/T \sim 10^2$, so that the high frequency behavior described above should be relevant. The crossover modulus between the high and intermediate frequency regimes is $G_2 \sim 10$ Pa. Long-time *fluidification* is also clear: relaxation times for coils ($L = 50$ μm) and rod-like polymers ($L = 5$ μm) are, respectively, $t_3 \sim 1$ s and $t_4 \sim 0.1$ s, compared to $t_3 \sim 10^4$ s and $t_4 \sim 100$ s for passive solutions at the same actin concentration. The corresponding plateau are, respectively, $G_3 \sim 10^{-2}$ Pa and $G_4 \sim 10^{-4}$ Pa.

In this Letter we have considered the driven dynamics of actin filaments using a modified tube model. This picture is valid only within certain limits: When motors stall at polymer ends before detaching [4] and at high concentration of motors we expect formation of statically inhomogeneous structures. We do note, however, that both analytic [5] theories of coupled motor/filament systems and simulations [3] have *neglected* entanglement; they have surely *underestimated* the dynamic stability of actin-myosin systems where the filaments are strongly entangled. The criteria for stability of such systems is a difficult open problem.

In order to approximate the effect of the individual clusters of myosin by independent, short duration impulses we require that neighboring clusters on the same filament do not see each other via tension propagation, implying that $\ell_m > \ell_\parallel$. This criterion is verified in the regime that we have discussed. Finally, our calculation was inspired by the observation of fluidification of an actin-myosin solution. However, this system could "fluidify" in other ways: Myosin, in the absence of ATP acts as a passive cross-linker. The sudden addition of ATP can lead to a rupture of the network, breakage of filaments, and thus fluidification. An alternative scenario is that polymers could buckle out of their tubes due to spatially inhomogeneous motility, leading to hernias and thus increased entanglement.

We thank F. Amblard, E. Furst, D. Humphreys, J. Käs, L. Le Goff, and J. Prost for discussions. The financial support of the European Union under Marie Curie Research Grant No. FMBICT972699 and the Royal Society is gratefully acknowledged (T. B. L.).

[1] J. Howard, Nature (London) **389**, 561 (1997).
[2] D. Humphreys and J. Käs (unpublished).
[3] F. Nedelec *et al.,* Nature (London) **389**, 305 (1997).
[4] F. Nedelec, Ph.D. thesis, Université Paris XI, 1998.
[5] K. Kruse and F. Jülicher, Phys. Rev. Lett. **85**, 1778 (2000).
[6] J. Prost (unpublished).
[7] M. Doi and S. F. Edwards, *The Theory of Polymer Dynamics* (Clarendon, Oxford, 1992).
[8] S. A. Langer and A. J. Liu, Europhys. Lett. **49**, 68 (2000).
[9] H. Isambert and A. C. Maggs, Macromolecules **29**, 1036 (1996).
[10] F. C. MacKintosh, J. Käs, and P. A. Janmey, Phys. Rev. Lett. **75**, 4425 (1995).
[11] A. C. Maggs, Phys. Rev. E **57**, 2091 (1998).
[12] D. Morse, Macromolecules **31**, 7030 (1998); **31**, 7044 (1998).
[13] F. Gittes and F. C. MacKintosh, Phys. Rev. E **58**, R1241 (1998).
[14] T. Odijk, Macromolecules **16**, 1340 (1983).
[15] M. Doi, J. Polym. Sci. Polym. Symp. **73**, 93 (1985).
[16] A. N. Semenov, J. Chem. Soc. Faraday Trans. **2**, 317 (1986).
[17] T. B. Liverpool and A. C. Maggs (to be published).
[18] R. Everaers *et al.,* Phys. Rev. Lett. **82**, 3717 (1999).